

Preprint PFC/JA-81-2

THE DIFFUSIVE WIGGLER - A SPATIALLY PERIODIC
MAGNETIC PUMP FOR FREE-ELECTRON LASERS

K. D. Jacobs and G. Bekefi

Massachusetts Institute of Technology
Cambridge, Massachusetts 02139

and

J. R. Freeman

Sandia Laboratories
Albuquerque, New Mexico 87115

January 1981

THE DIFFUSIVE WIGGLER - A SPATIALLY PERIODIC MAGNETIC
PUMP FOR FREE-ELECTRON LASERS

K. D. Jacobs and G. Bekefi

Department of Physics and Research Laboratory of Electronics
Massachusetts Institute of Technology
Cambridge, Massachusetts 02139

and

J. R. Freeman

Sandia Laboratories
Albuquerque, New Mexico 87115

ABSTRACT

Magnetic diffusion through a spatially periodic assembly of metal conductors yields a large amplitude, quasi-static pump for use in free-electron lasers. The experimental observations are compared with predictions of a 2-D triangular mesh, finite difference magnetic diffusion code (TRIDIF).

I. INTRODUCTION

The relativistic electron beam of a magnetically pumped free-electron laser¹⁻⁴ is subjected to two external fields: a uniform, axial magnetic field which guides the beam, and a transverse, quasi-static, periodic magnetic field which causes stimulated Compton² or Raman³ scattering in the drifting electrons. The two fields are produced independently of one another and are driven by separate power sources. Typically, the guiding field is furnished by a solenoid, and the magnetic "wiggler" field is obtained by passing current through helical windings^{2,5,6,7,8} or through a series of metal rings⁴ inserted in the solenoid and surrounding the electron beam. In order to achieve interesting levels of coherent radiation in the millimeter or submillimeter range of wavelengths, one must strive for large wiggler amplitudes B_1 and small wiggler periodicities λ . The simultaneous requirement of a large B_1 and a small λ is technically difficult, and the largest value of the ratio B_1/λ achieved to date is $\sim 800\text{G/cm}$ with $0.6 \leq \lambda \leq 3.2\text{cm}$. In section II below we describe a novel type of "diffusive" wiggler⁹ which is simple and efficient. Only a single power source is needed to generate both the guiding magnetic field and the transverse wiggler field.

II. EXPERIMENTS AND COMPUTATIONS

As is illustrated in Fig. 1, the relativistic electron beam propagates down a drift tube surrounded by a solenoid containing a periodic assembly of copper rings¹⁰ separated by electrically insulating rings. If the current through the solenoid is time varying, then the solenoid field will diffuse gradually through the copper rings, but will quickly penetrate the insulating rings.

This will give rise to a spatially modulated magnetic field in the region of the electron beam. We present here the results of detailed experimental studies and numerical computations of the temporal and spatial distribution of magnetic fields in our diffusive wiggler pump.

The experiments were carried out using a 92cm long, 30mH solenoid having 25 turns per centimeter length, and able to accommodate rings with a maximum radius of 3.3cm. The solenoid is powered by a 3.75mF capacitor bank which can be charged to a maximum of 4kV, giving a peak current of 720A. The current pulse through the solenoid is a half sine wave of frequency 16Hz, and is measured using a 0.010 Ω resistive shunt.

Both the radial and axial magnetic fields are measured for a variety of ring periodicities λ , and ring radial wall thicknesses W . The fields are measured using a gaussmeter and Hall effect probes. The probe elements are approximately 2mm square in a plane perpendicular to the field, and extend less than 0.05mm along the field. Since the fields vary on the scale of a few centimeters, spatial averaging of the fields due to the finite probe size can be neglected. The gaussmeter is able to follow the instantaneous magnetic field to within 2% at the 16Hz characteristic frequency of our system. The overall uncertainty in the measurements is approximately 5%.

To check the experimental results and then establish the scaling of the field modulation with the ring thickness W , periodicity λ and the solenoid current risetime, a 2-D triangular mesh finite-difference magnetic diffusion code entitled TRIDIF^{1,1} has been used. TRIDIF is a modification of the PANDIRA-SUPERFISH^{1,2} code which

was designed to compute transient magnetic field diffusion and eddy current problems. The code solves the usual diffusion equation for the magnetic vector potential,

$$\mu_0 \sigma \frac{\partial \vec{A}}{\partial t} = -\nabla \times (\nabla \times \vec{A}) + \mu_0 \vec{J}_s ,$$

where \vec{J}_s is a source current density produced within the solenoid windings and σ is the conductivity of the medium. An example of the computational mesh used for the $\ell=2\text{cm}$, $W=1.1\text{cm}$ case is shown in Fig. 2. Figure 3 displays the computed field lines at $t=2.0\text{ms}$, early in the current risetime of 15ms . The boundary conditions used in the calculation were $\partial\psi_\theta/\partial n=0$ at all boundaries, where $\psi_\theta = rA_\theta$ is the azimuthal magnetic stream function.

The utility of the above approach was first established by comparing the computer results with all of the available experimental data for these configurations. In these comparisons, the measured time-dependent solenoid current shown in Fig. 4 was used as input to the code. No normalizations or time-shifts were required. The solenoid was modeled by a simple, thin, uniform current density shell located at the radius of 3.77cm . Due to the cylindrical symmetry of the ring assembly, the radial field B_r is zero on axis. Thus, for free-electron laser applications, an annular electron beam is required. Consequently, all fields were measured and computed off axis. We have chosen a radius $r=0.86\text{cm}$, which represents the "beam position" of Figs. 2 and 3.

Figure 4 shows the temporal behavior of the magnetic fields, and Fig. 5 illustrates their spatial behavior for the case where the periodicity $\ell=4\text{cm}$ and the ring thickness $W=2.1\text{cm}$. In Fig. 5,

the results are plotted at time $t=10\text{ms}$, the time when the radial field modulation was maximum (see Fig. 4). The solid curves are the measured data, and the dots denote the computed results. Excellent agreement is observed. Note that the field is primarily axial. Thus, the same solenoid used to produce the periodic radial field B_r also provides the guiding magnetic field B_z . (The amplitude modulation of B_z does not participate in the free-electron laser interaction.)

Information on the scaling of the peak field modulation at $r=0.86\text{cm}$ with the width W and periodicity ℓ was obtained by making measurements on experimental assemblies for $\ell=2,4,6$, and 8cm and $W=1.1$ and 2.1cm . Experimentally, the pump period ℓ is varied simply by arranging the rings in a different order. The results are shown as solid ($W=2.1$) and broken ($W=1.1$) curves in Fig. 6. The TRIDIF computations are shown as solid ($W=2.1$) and hollow ($W=1.1$) dots. The comparison is again seen to be quite good over a considerable range of periodicity and width.

An experiment was also performed with an adiabatic field shaper designed to increase the transverse field modulation more gradually¹ at the beam injection end of the solenoid. This is readily accomplished by decreasing the thickness W of the first one (or more) rings as is illustrated in Fig. 7. Figure 8 shows the measured and computed spatial field distributions in the vicinity of the field shaper at $t=10\text{ms}$. The agreement between experiment and computations is seen to be good except for small values of z where the computed axial magnetic field B_z is larger than the measured field by about 12%. This discrepancy is due to fringing field effects neglected in the computations. In the

experiments the axial position $z = 0$ shown in Fig. 8 is - 7 cm from the end of the solenoid. Using this value, we can account for a discrepancy of $\sim 10\%$. However, this is not a serious problem, since the quantity of interest, the radial magnetic field modulation B_r is predicted with good accuracy.

We see from Fig. 8 that the axial magnetic field B_z outside the region occupied by the copper rings is almost twice as large as the spatially averaged B_z inside the rings. Thus the electron gun stationed near the origin $z=0$ is immersed in a much stronger axial field than that occurring in the interaction region of a free electron laser system. Consequently, on entering the interaction region, the electron beam expands radially. This causes a "cooling" of the beam (the radial electron energy decreases) and is advantageous to the operation of the laser.

TRIDIF was next used to predict additional scaling over a wide range of ring periodicity ℓ and wall thickness W as shown in Fig. 9. A 15ms solenoid current risetime was used for all cases. The time of peak field modulation was found to vary significantly with respect to the time of peak current, with larger values of W peaking later in time than smaller values. This feature is caused by the longer time required for the field to diffuse from the outside to the inside of the thicker rings.

The predicted scaling with the solenoid current risetime T is shown in Fig. 10 for a fixed periodicity of $\ell=2\text{cm}$. Since the optimum thickness for a given periodicity and risetime is of the order of one skin depth $\delta=(T/\pi\mu_0\sigma)^{1/2}$, smaller values of W require shorter risetimes for best performance. The dependence of this

optimum on the risetime T is fairly weak, since $\delta \sim T^{1/2}$. The effects of diffusion in the coil could affect these results for thick solenoids and short risetimes.

III. CONCLUSIONS

The diffusive wiggler described above is a simple, passive system in which the pulsed solenoid provides both the guiding axial magnetic field and the transverse periodic pump field. The achievable pump amplitudes are large as can be seen from Fig. 6 and 8. To obtain even larger amplitudes, one can increase the solenoid current from the nominal value of 720A used in the experiments. (The amplitude increases linearly with current.) For purposes of comparison we note that an "active" helical wiggler⁸ having a radius of 1.7cm and a period λ of 2cm gives a transverse field of 21G on axis ($r=0$) and ~ 100 G at $r=0.8$ cm, per kiloampere of current flowing through its windings.

The ripple periodicity λ is readily changed in a diffusive wiggler merely by rearranging the way the copper and insulating rings are stacked. We note that the fields change on a time scale of milliseconds. This means that during the short time (tens of nanoseconds to microseconds) a typical pulsed, relativistic electron beam is on, the magnetic fields are essentially constant. Thus, by varying the time during the magnet pulse at which the beam pulse is turned on, and by varying the charging voltage on the solenoid capacitor bank, the radial field B_r and the spatially averaged axial field B_z can be varied at will, independently of each other. We have also shown that a beam shaper is readily constructed by slowly varying the ring thickness W of the first

few rings. This allows adiabatic injection¹ of the electron beam into the interaction region. We note that the construction of a beam shaper with active helical windings is technically difficult.

The excellent agreement of experiment with the TRIDIF computer code gives one confidence as to its reliability in computing magnetic fields in parameter regimes (Figs. 9 and 10) that have not been explored experimentally.

ACKNOWLEDGEMENTS

This work was supported in part by the U.S. Air Force Office of Scientific Research and in part by the National Science Foundation.

REFERENCES

1. P. Sprangle, R.A. Smith, and V.L. Granatstein, Naval Research Laboratory Report No. 3911 (unpublished, 1978), and bibliography therein.
2. L.R. Elias, W.M. Fairbank, J.M.J. Madey, H.A. Schwettman, and T.I. Smith, Phys. Rev. Lett. 36, 717 (1976); D.A.G. Deacon, L.R. Elias, J.M.J. Madey, G.J. Ramian, H.A. Schwettman, and T.I. Smith, *ibid.* 38, 892 (1977).
3. V.L. Granatstein, S.P. Schlesinger, M. Herndon, R.K. Parker, and J.A. Pasour, Appl. Phys. Lett. 30, 384 (1977).
4. D.B. McDermott, T.C. Marshall, S.P. Schlesinger, R.K. Parker, and V.L. Granatstein, Phys. Rev. Lett. 41, 1368 (1978).
5. B.M. Kincaid, J. App. Phys. 48, 2684 (1977).
6. J.P. Blewett and R. Chasman, J. Appl. Phys. 48, 2692 (1977).
7. J.M. Buzzi, K. Felch, and L. Vallier, Bull. Am. Phys. Soc. 25, 887 (1980).
8. J.M. Buzzi, K. Felch, and L. Vallier, Laboratoire de Physique des Milieux Ionises, Ecole Polytechnique, Palaiseau, France Report No. PMI 1008 (1980).
9. K.D. Jacobs, R.E. Shefer, and G. Bekefi, Appl. Phys. Lett. 37, 583 (1980).
10. The use of a periodic assembly of iron rings has been reported by P.C. Efthimion and S.P. Schlesinger, Phys. Rev. A16, 633 (1977); R.M. Gilgenbach, T.C. Marshall, and S.P. Schlesinger, Phys. Fluids 22, 971 (1979). However, because of effects caused by magnetic saturation and hysteresis in iron, this technique is not entirely satisfactory.
11. J.R. Freeman, J. Comp. Phys. (to be published).

12. K. Halbach and R.F. Holsinger, Particle Accel. 7, 213 (1976).

CAPTIONS TO FIGURES

- Fig. 1. Sketch of a diffusive wiggler pump of periodicity ℓ and ring thickness W (W is of the order of a skin depth $\delta = (T/\pi\mu_0\sigma)^{1/2}$ where T is the rise time of the solenoid current). The first ring is smaller and comprises the adiabatic field shaper. The spaces between the copper rings are occupied by Plexiglass rings.
- Fig. 2. Cross-section of the wiggler overlaid with the computational mesh, for the case $\ell=2\text{cm}$, $W=1.1\text{cm}$.
- Fig. 3. Computed magnetic field lines at a time $t=2\text{ms}$ after pulsing on the current through the solenoid ($\ell=2\text{cm}$, $W=1.1\text{cm}$, $I_{\text{max}}=720\text{A}$).
- Fig. 4. Time development of the solenoid current, and the radial and axial magnetic fields at $r=0.86\text{cm}$ ($\ell=4\text{cm}$, $W=2.1\text{cm}$, $I_{\text{max}}=720\text{A}$). The solid lines are from measurements, the dots are from TRIDIF.
- Fig. 5. Axial distribution of the magnetic fields at $r=0.86\text{cm}$, for the case $\ell=4\text{cm}$, $W=2.1\text{cm}$, at a time $t=10\text{ms}$ at which the radial field modulation is maximum. The solid lines are from measurements, the dots are from TRIDIF.
- Fig. 6. The radial magnetic field amplitude as a function of the wiggler periodicity ℓ , for two values W , at times t at which B_r is maximum. The lines are from measurements, the dots and open circles from TRIDIF ($r=0.86\text{cm}$, $I_{\text{max}}=720\text{A}$).
- Fig. 7. The field lines in the vicinity of the adiabatic field shaper ($t=5\text{ms}$, $\ell=6\text{cm}$). The dashed line represents the "beam position" $r=0.86\text{cm}$.

- Fig. 8. Axial distribution of the magnetic fields in the vicinity of the field shaper ($t=10\text{ms}$, $l=6\text{cm}$, $r=0.86\text{cm}$). The solid lines are from measurements, the dots from TRIDIF.
- Fig. 9. Computed radial magnetic field amplitude as a function of ring thickness W , for several values of the periodicity l , at a time t when B_r is maximum. The current rise time is 15ms ; $I_{\text{max}} = 720\text{A}$; δ is the skin depth.
- Fig. 10. Computed radial magnetic field amplitude as a function of the rise time of the current in the solenoid for different values of W , at a time t when B_r is maximum ($l=2\text{cm}$, $I_{\text{max}} = 720\text{A}$).

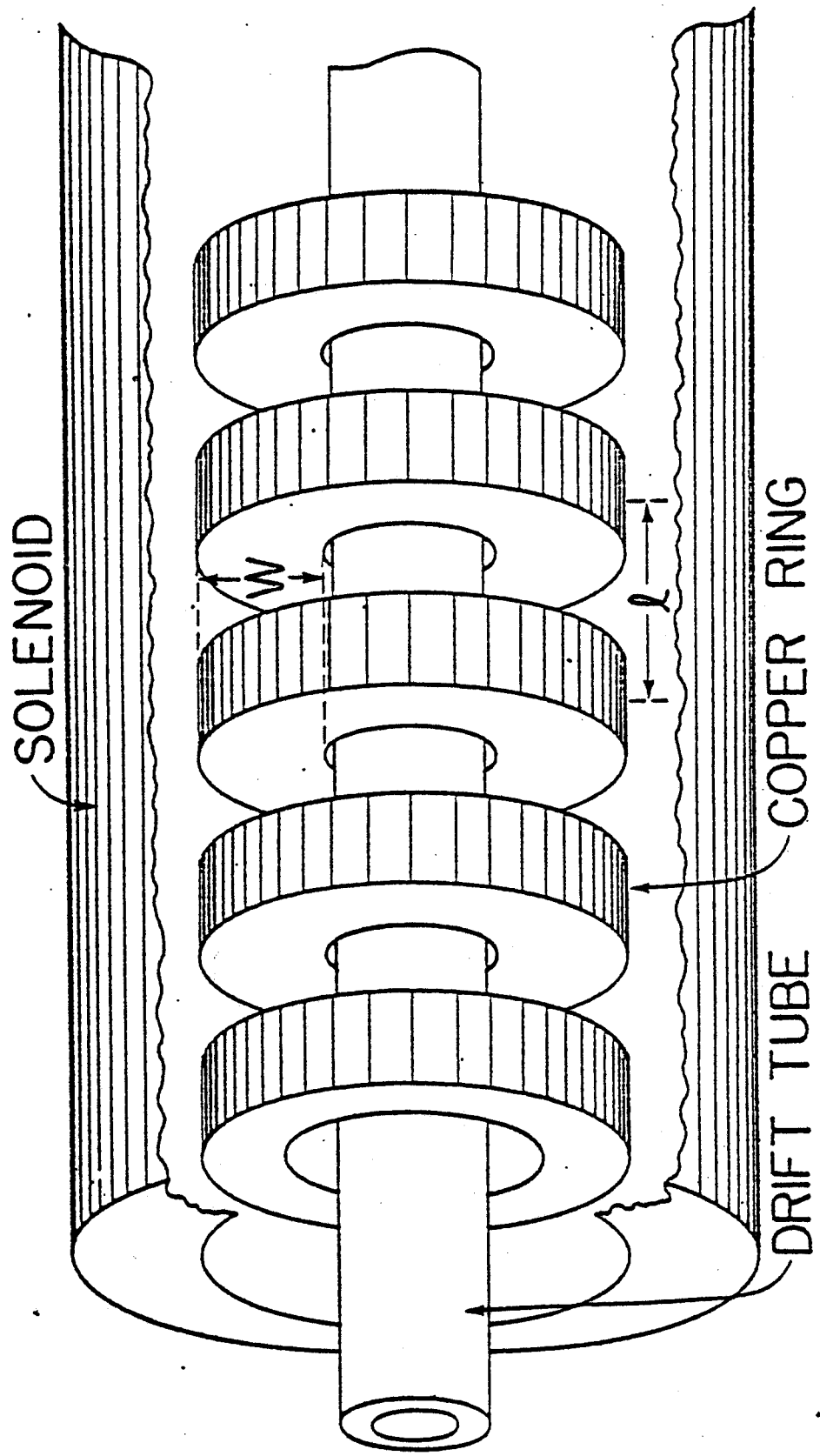


Fig. 1
Jacobs, Bekefi, & Freeman

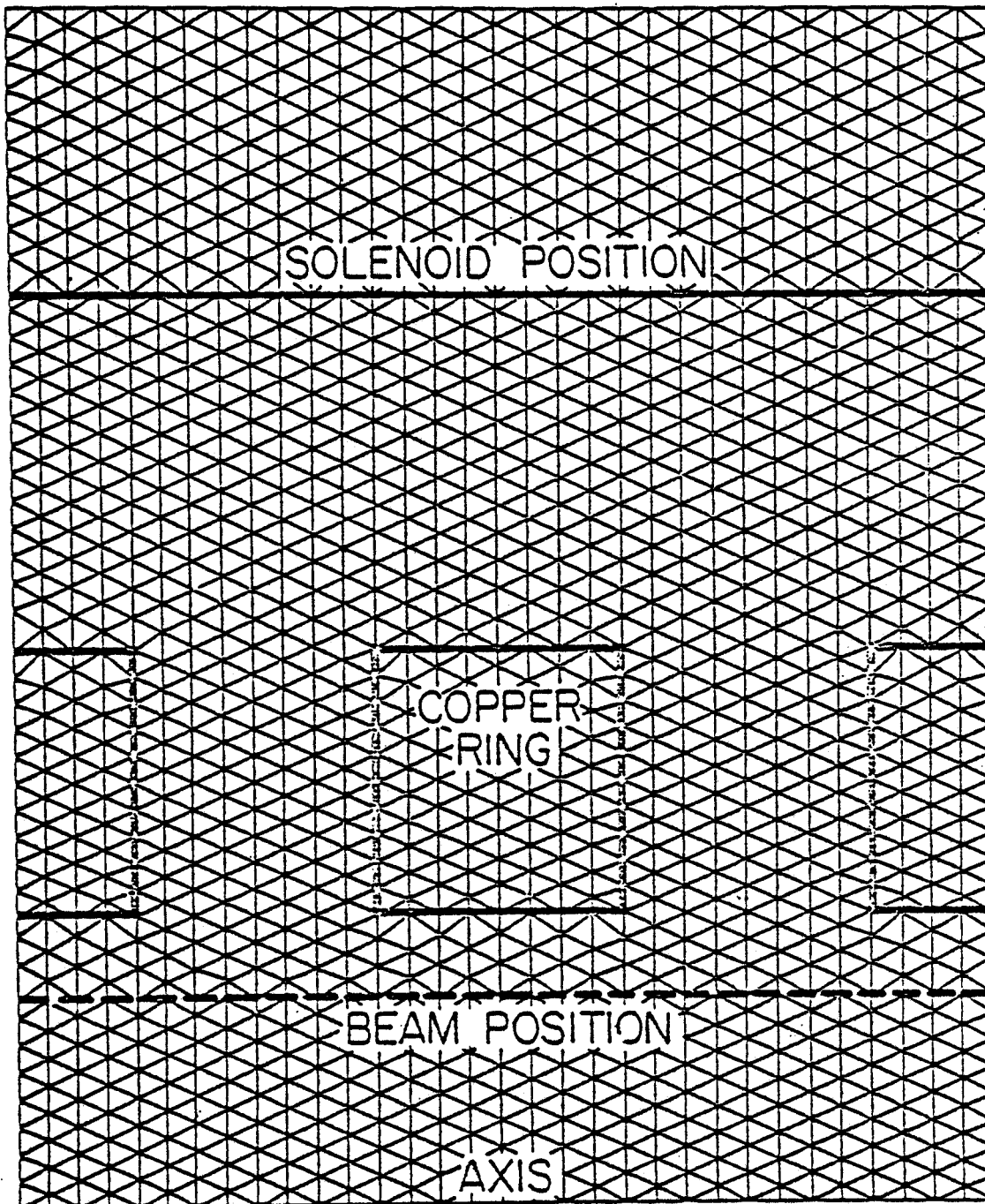


Fig. 2
Jacobs, Bekafi, & Freeman

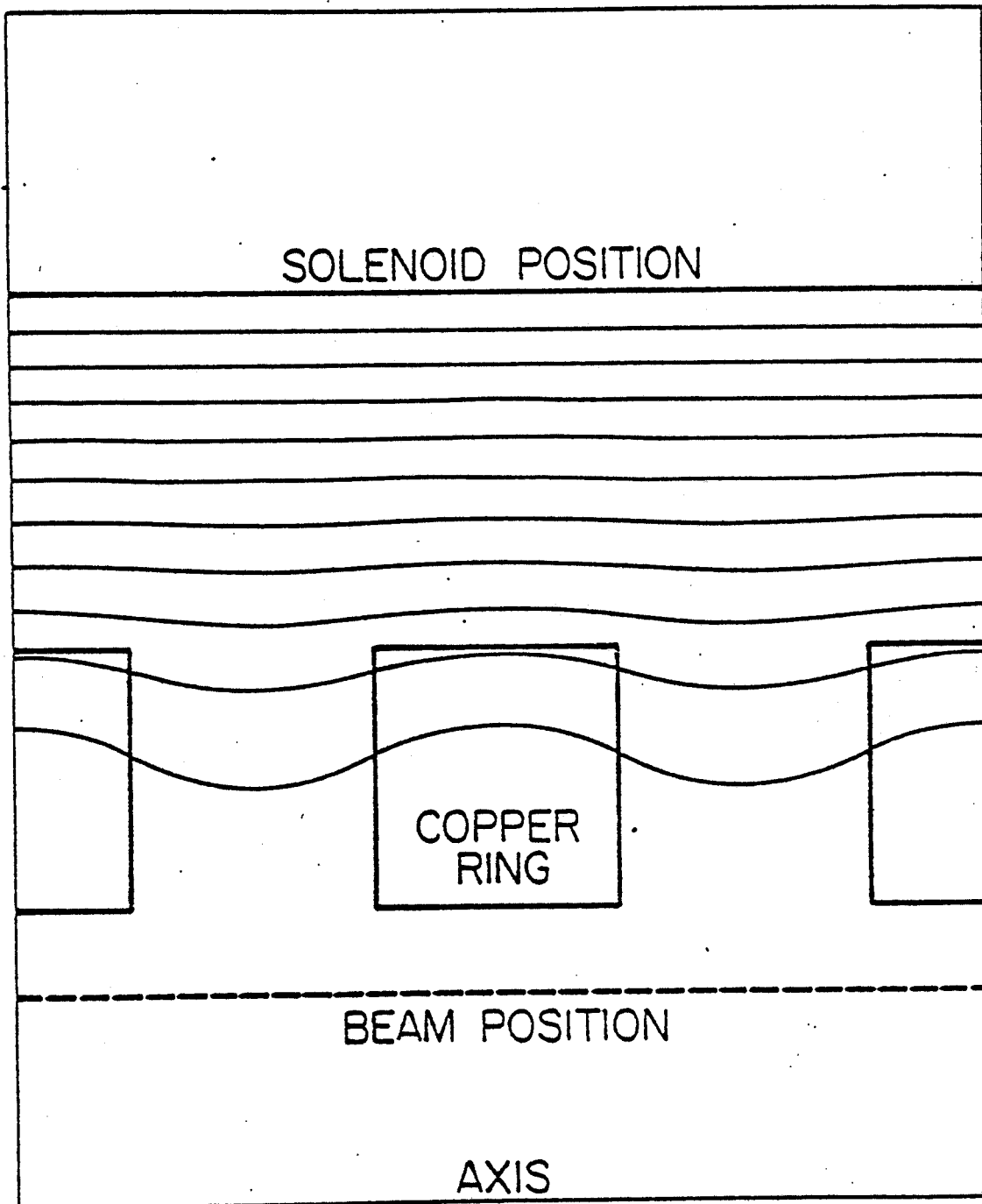


Fig. 3
Jacobs, Bekefi, & Freeman

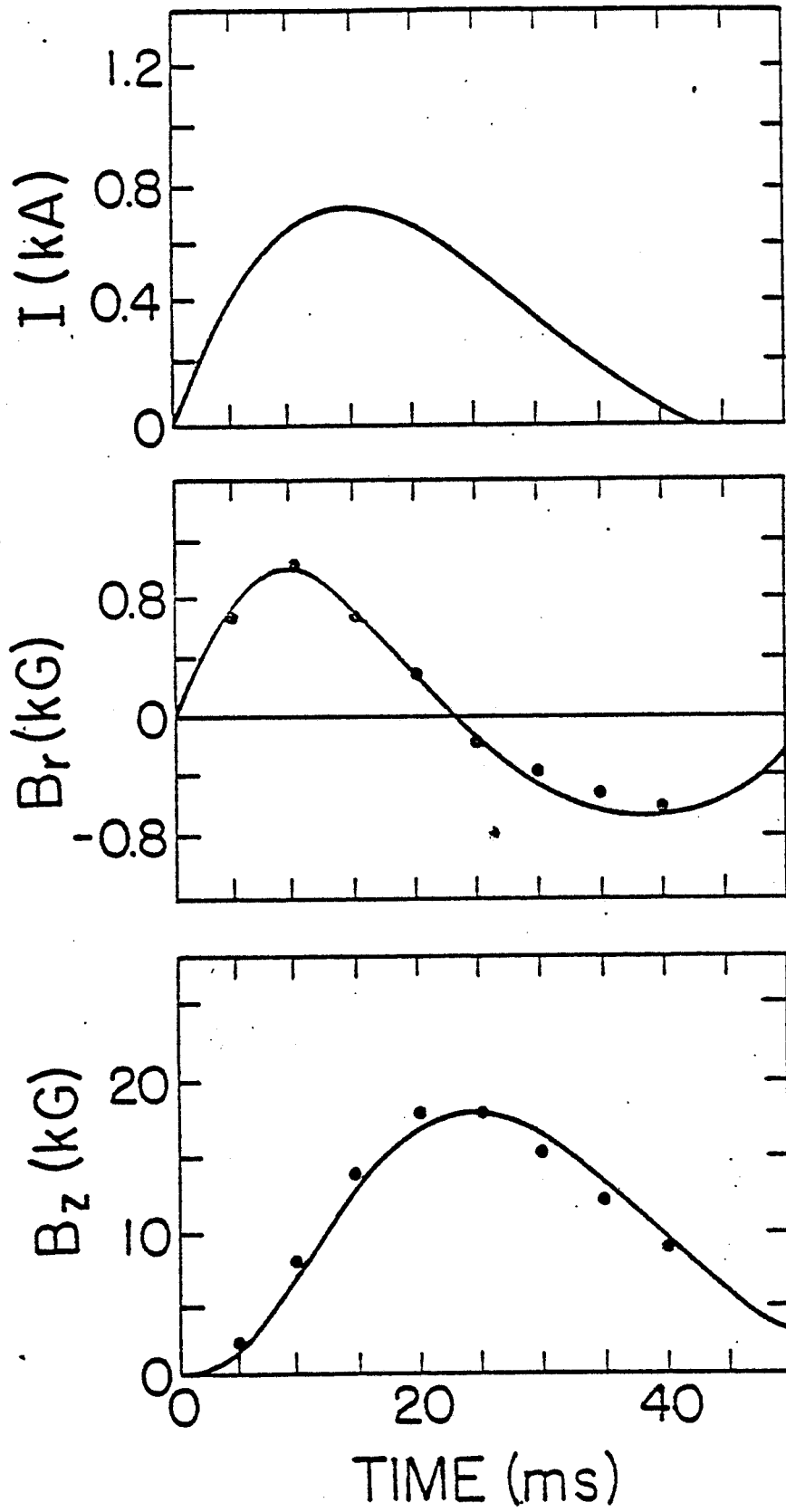


Fig. 4
Jacobs, Bekefi, & Freeman

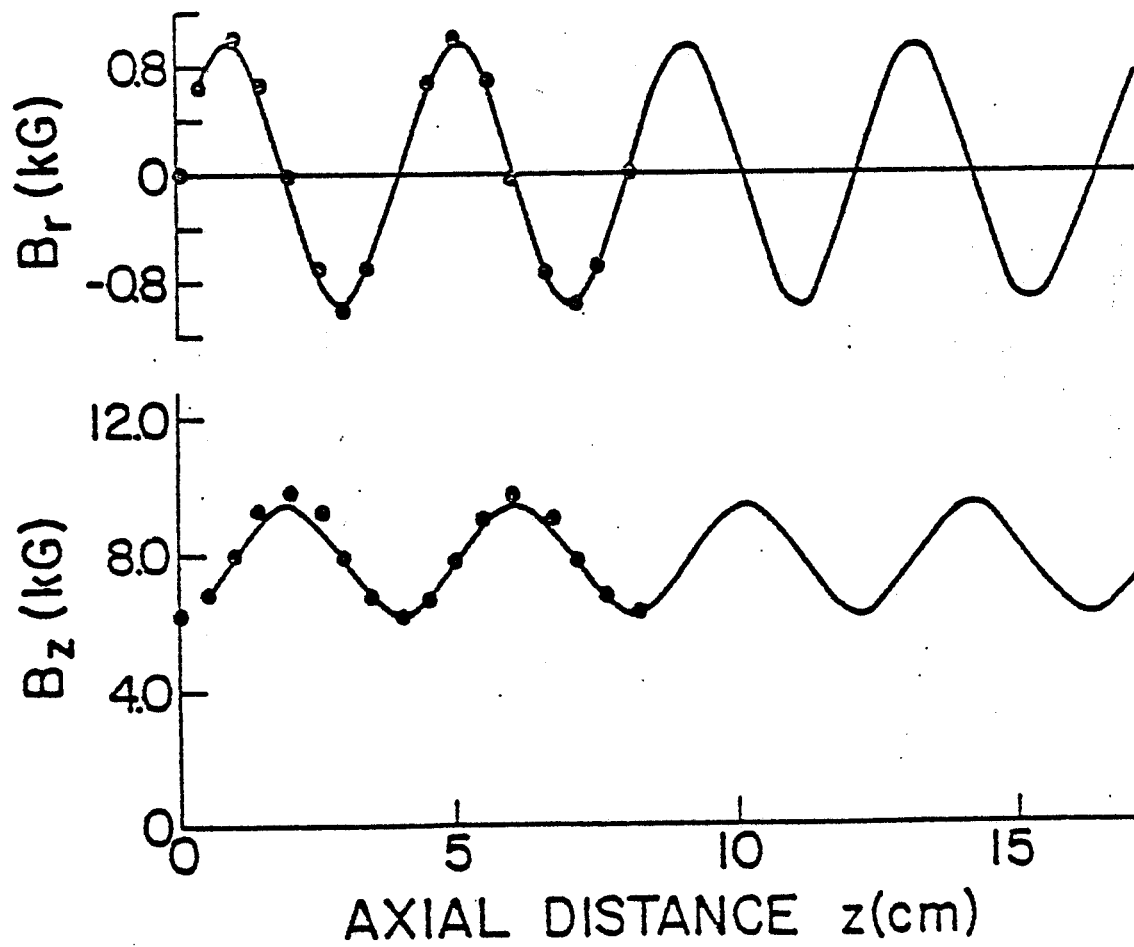
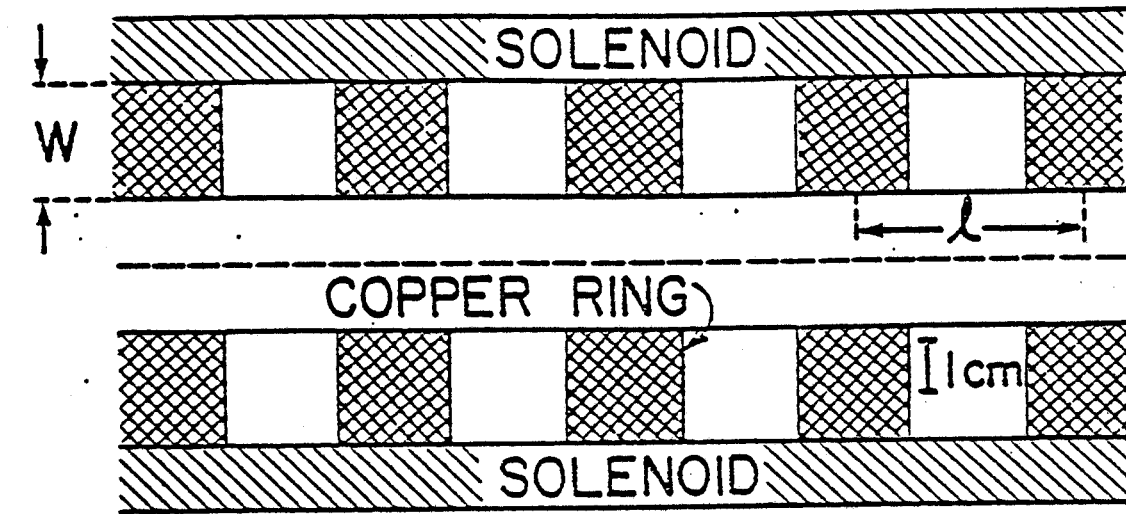


Fig. 5
Jacobs, Bekefi, & Freeman

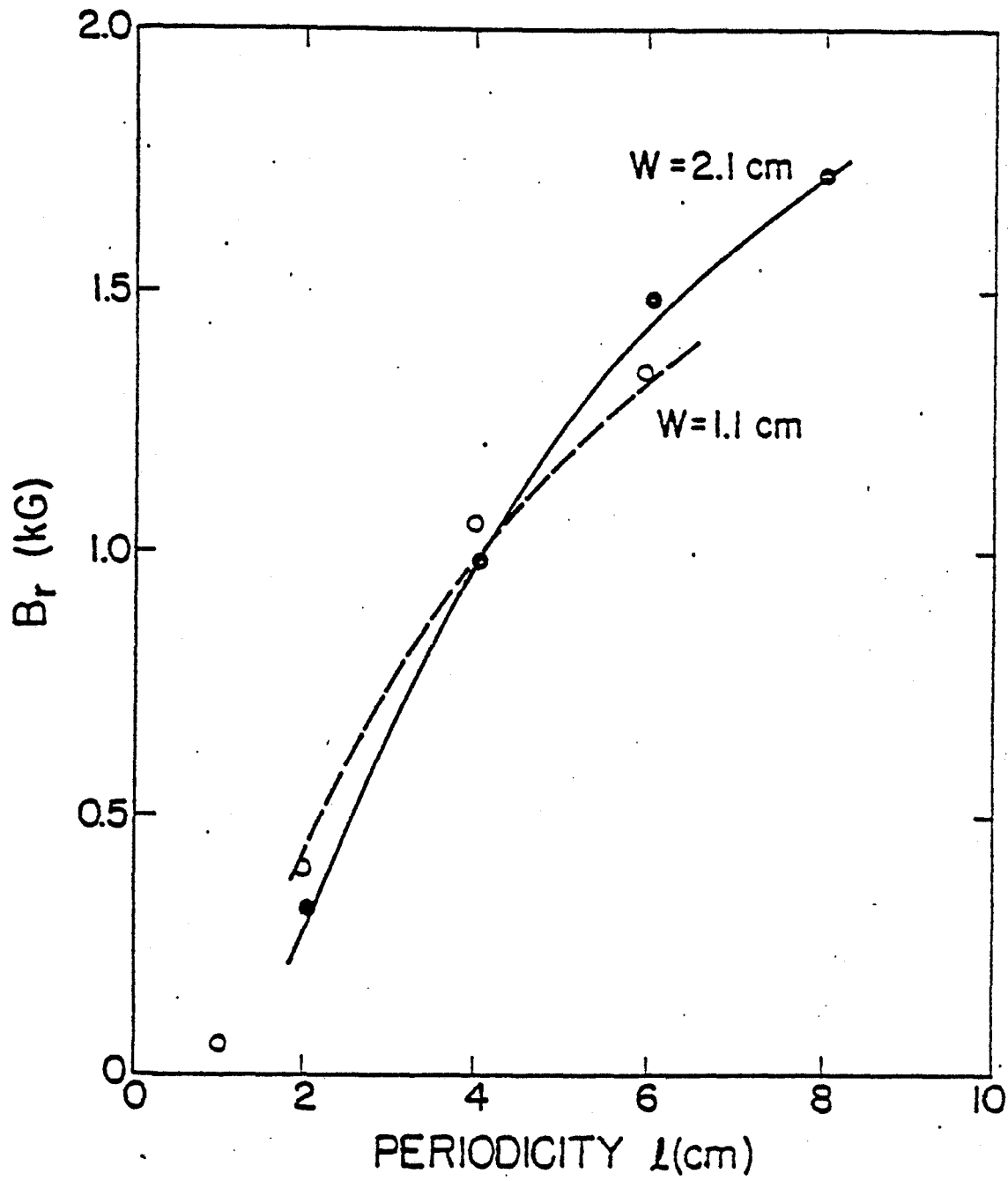
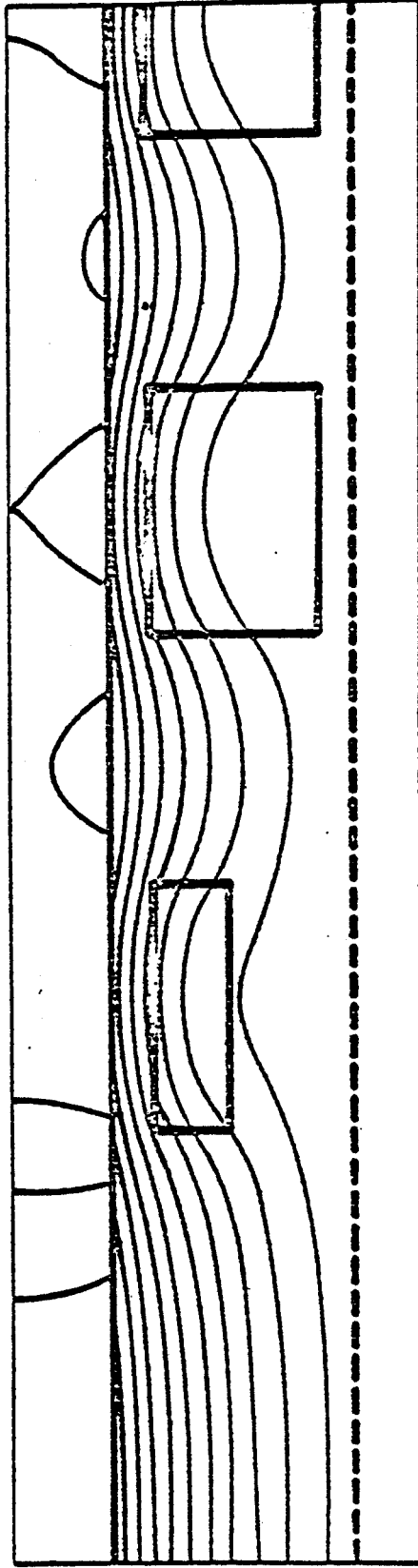


Fig. 6
Jacobs, Bekefi, & Freema



AXIS

Fig. 7
Jacobs, Bekefi, & Freeman

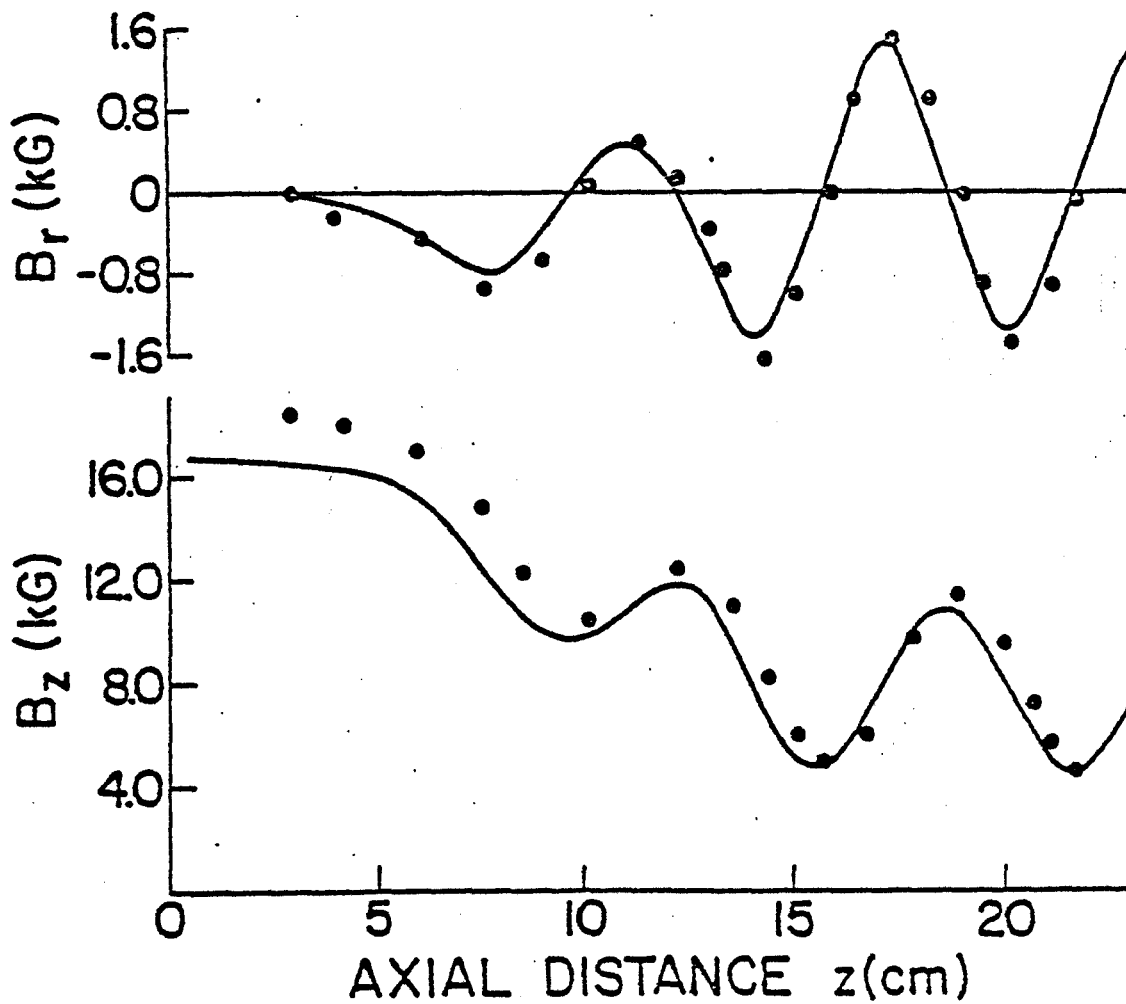
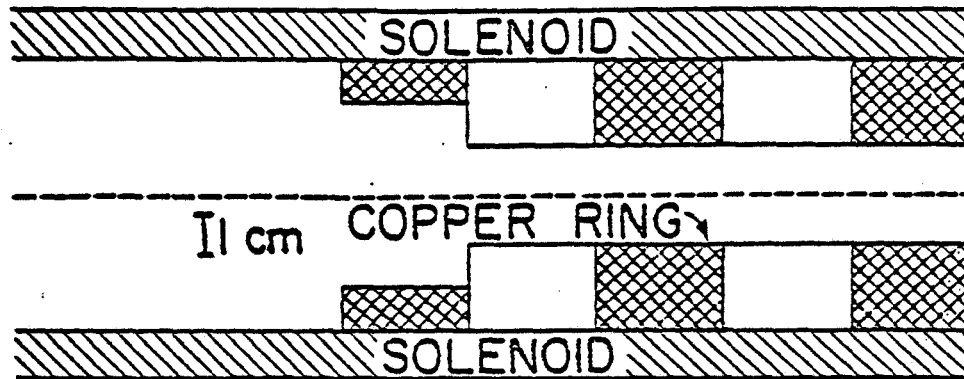


Fig. 8
Jacobs, Bekefi, & Freeman

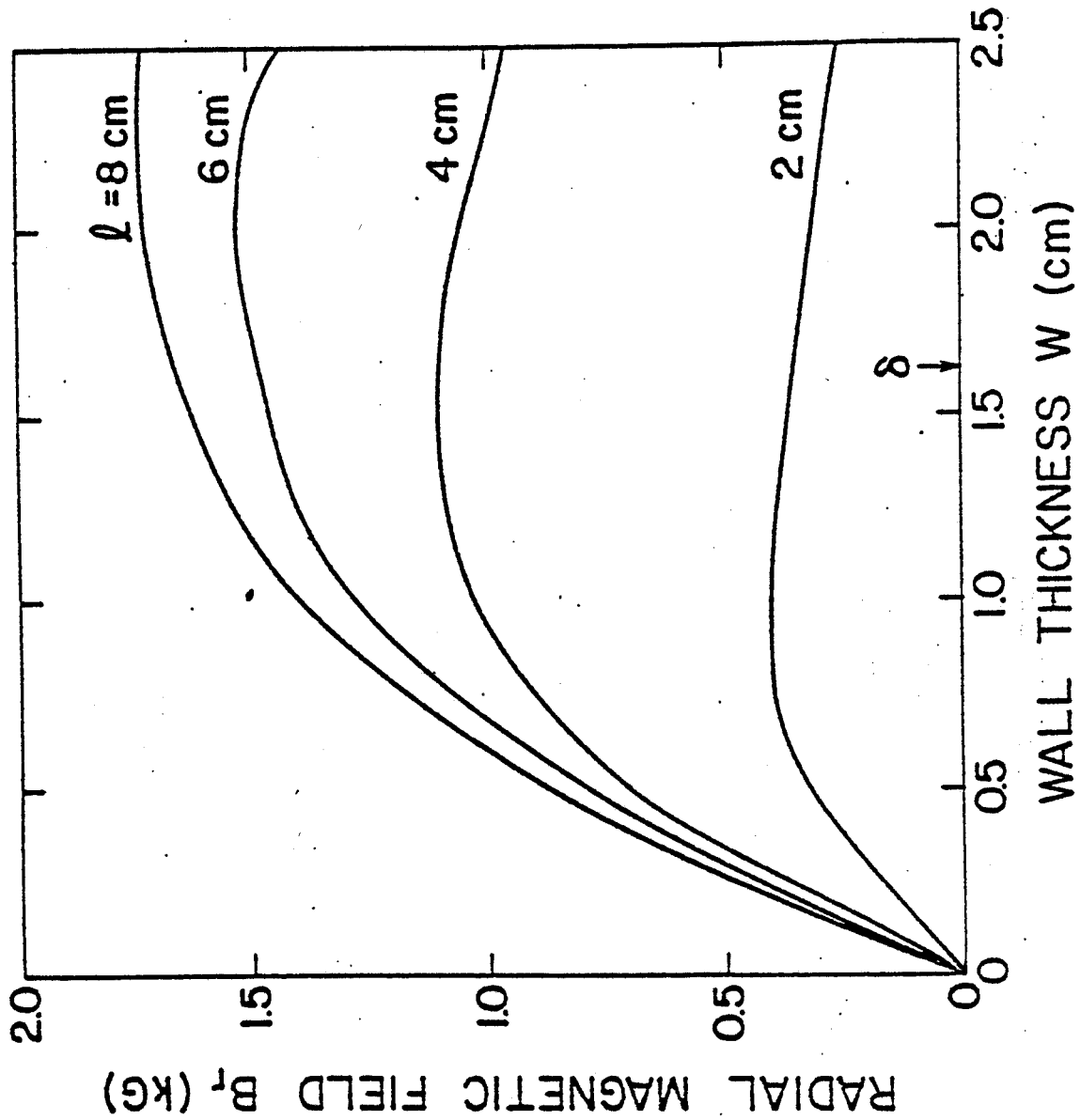


Fig. 9
Jacobs, Bekefi, & Freeman

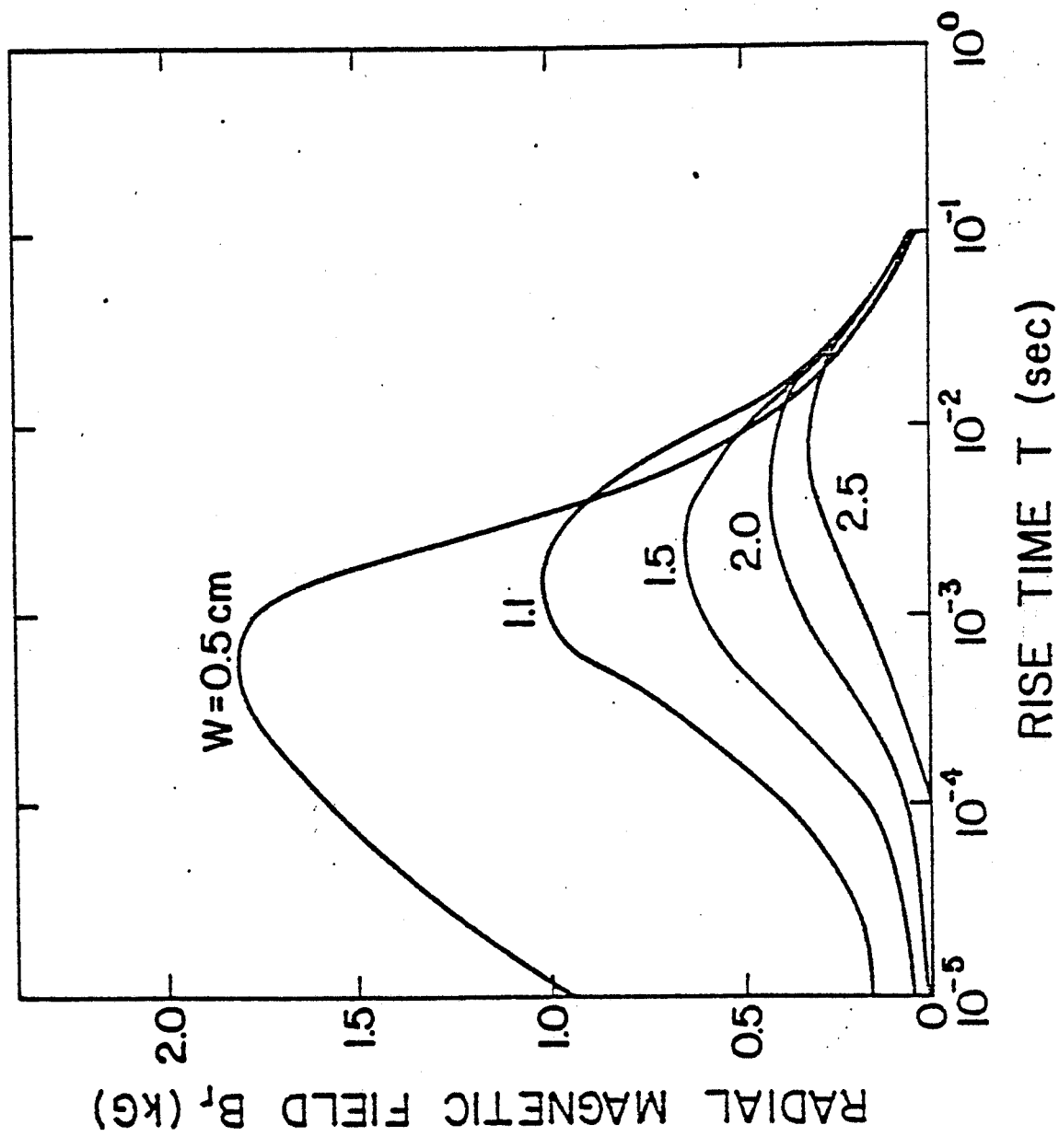


Fig. 10
Jacobs, Bekefi, & Freeman